

AMS subject classifications. 65K10, 65F08, 65F15

**PRECONDITIONING ORBITAL MINIMIZATION METHOD FOR PLANEWAVE
DISCRETIZATION**

JIANFENG LU AND HAIZHAO YANG

ABSTRACT. We present an efficient preconditioner for the orbital minimization method when the Hamiltonian is discretized using planewaves (i.e., pseudospectral method). This novel preconditioner is based on an approximate Fermi operator projection by pole expansion, combined with the sparsifying preconditioner to efficiently evaluate the pole expansion for a wide range of Hamiltonian operators. Numerical results validate the performance of the new preconditioner for the orbital minimization method, in particular, the iteration number is reduced to $\mathcal{O}(1)$ and often only a few iterations are enough for convergence.

1. INTRODUCTION

We consider the problem of finding the low-lying eigenspace of a Hamiltonian matrix H coming from the planewave discretization of a self-adjoint Hamiltonian operator $-\frac{1}{2}\Delta + V$ for some potential function V . Given an $n \times n$ Hamiltonian matrix H , it is well-known that, the eigenspace associated to the first N eigenvalues (non-degeneracy is assumed throughout the work) is given by the trace minimization

$$(1) \quad E = \min_{X \in \mathbb{C}^{n \times N}, X^* X = I_N} \frac{1}{2} \operatorname{tr}(X^* H X),$$

where I_N is a $N \times N$ identity matrix, thus $X^* X = I_N$ is the orthonormality constraints of the columns of X . When a conventional algorithm is used to solve for the eigenvalue problem, a QR factorization in each iteration is required to impose orthogonality. The computational cost of each QR is $\mathcal{O}(nN^2)$ with a large prefactor and communication cost is expensive in high performance computing. This creates an obstacle to minimize (1) if the number of iteration is large. Much effort has been devoted to reducing the communication cost, see e.g., [5, 18] and references therein.

It turns out that it is in fact possible to remove the orthogonality constraint. In the context of linear scaling algorithms for electronic structure calculations, the orbital minimization method (OMM) was proposed in [19–22] to circumvent the orthonormality constraint in (1). Instead, we search for the eigenspace by an unconstrained minimization

$$(2) \quad E = \min_{X \in \mathbb{C}^{n \times N}} E_{\text{omm}}(X) = \min_{X \in \mathbb{C}^{n \times N}} \frac{1}{2} \operatorname{tr}((2I_N - X^* X)(X^* H X)).$$

Date: October 24, 2018.

Key words and phrases. Kohn-Sham density functional theory, orbital minimization method, preconditioning, Fermi operator projection, pole expansion, sparsifying preconditioner.

This work is partially supported by the National Science Foundation under grants DMS-1312659, DMS-1454939, and ACI-1450280. H.Y. thanks the support of the AMS-Simons Travel Award. We thank Lexing Ying for helpful discussions.

To see where (2) comes from, notice that we may reformulate (1) to relax the orthogonality constraint as

$$(3) \quad E = \min_{X \in \mathbb{C}^{n \times N}, \text{rank } X = N} \frac{1}{2} \text{tr}((X^* X)^{-1} (X^* H X)),$$

so that X is no longer constrained. The factor $(2I_N - X^* X)$ in (2) can then be seen as a Neumann series expansion of $(X^* X)^{-1} = (I_N - (I_N - X^* X))^{-1}$ truncated to the second term.

Somewhat surprisingly, for negative definite H (all the eigenvalues are strictly less than 0), the minimizer of E_{omm} spans the same subspace as the minimizer to the original problem (1), thus the desired eigenspace [19, 20]. Note that the assumption that H being negative definite can be made without loss of generality, as we may just shift the diagonal of H by a constant, and this shift will not change the eigenspace.

The OMM was originally proposed for linear scaling calculations (the total computational cost is linearly proportional to N , the number of electrons) for sparse H , combined with truncating X to keep only $\mathcal{O}(1)$ entries per column. However, even without adopting the linear scaling truncation, whose error can be hard to control, in the context of cubic scaling implementation, the OMM algorithm still has advantage over direct eigensolver in terms of scalability in parallel implementations [3]. The OMM has the potential to be a competitive strategy for finding the eigenspace.

Since the OMM transforms the eigenvalue problem into an unconstrained minimization, the nonlinear conjugated gradient method is usually employed to minimize the energy (2). The efficiency of the OMM algorithm thus depends on the optimization scheme, which in turn crucially depends on the preconditioner.

In this work, we will consider H coming from a Fourier pseudospectral discretization of the Hamiltonian operator. The pseudospectral method typically requires minimal degree of freedoms for a given accuracy among standard discretizations and is also easy to implement using the fast Fourier transform (FFT), and hence widely used in the field physics and engineering literature. In the field of electronic structure calculation, it is known as the planewave discretization, which is arguably the most popular discretization scheme up-to-date.

While the importance of preconditioning for planewave discretization is well known and has been long recognized [30]; the preconditioner has been mostly limited to the type of shifted inverse Laplacian (more details later). A natural question is whether more efficient preconditioner can be designed.

We revisit the issue of preconditioning for planewave discretization. We propose a new preconditioner using an approximate Fermi operator projection based on the pole expansion (see e.g., [1, 7, 8, 15, 26]). Once constructed, the new preconditioner can be applied efficiently and reduces the number of iteration of the OMM to only a few. The resolvents involved in the pole expansion are solved iteratively using GMRES [29] combined with the recently developed sparsifying preconditioner [17, 31, 32]. Since only an approximate Fermi operator is required, the construction and application of preconditioner become quite efficient. Hence, the overall preconditioned OMM requires much less computational time compared to existing OMM algorithms for planewave discretizations.

This paper is organized as follows. In Section 2, existing preconditioned OMMs are introduced and analyzed to motivate the design of the new preconditioner. In Section 3, we construct the

new preconditioner base on the approximate Fermi operator projection and the sparsifying preconditioner. In Section 4, some numerical examples are provided to demonstrate the efficiency of the new preconditioner. We conclude with a discussion and some future work in Section 5.

2. PRECONDITIONED ORBITAL MINIMIZATION METHOD

2.1. Orbital minimization method. The orbital minimization method (OMM) has become a popular tool in electronic structure calculations for solving the Kohn-Sham eigenvalue problem. One of the major advantage is that unlike conventional methods for eigenvalue calculations, no orthogonalization is required in the iteration. The OMM minimizes the functional E_{omm} , recalled here:

$$E = \min_{X \in \mathbb{C}^{N \times N}} E_{\text{omm}}(X) = \min_{X \in \mathbb{C}^{N \times N}} \frac{1}{2} \text{tr}((2I_N - X^* X)(X^* H X)).$$

The nonlinear conjugate gradient method is usually applied for this unconstrained minimization problem. When the minimization problem becomes ill-conditioned (for example, when the spectral gap, the difference between the N -th and $(N + 1)$ -th eigenvalues, is small; further discussed below), it requires a large number of iterations to achieve convergence. Hence, an efficient preconditioner is crucial to this minimization problem.

Let us consider preconditioning the gradient of E_{omm} in the general framework of nonlinear conjugate gradient methods. Denote the gradient as

$$(4) \quad \mathcal{G}(X) := \frac{\delta E_{\text{omm}}(X)}{\delta X^*} = 2HX - X(X^* H X) - HX(X^* X).$$

The preconditioned nonlinear conjugate gradient method can be summarized as follows.

<ol style="list-style-type: none"> 1 Initialize: Pick initial guess X_1 and fix a preconditioner \mathcal{P}; 2 Set $D_1 = -\mathcal{P}\mathcal{G}(X_1)$ and perform a line search in the direction of D_1 and update X_2; 3 Set $m = 2$; 4 while <i>not converged</i> do 5 Calculate the preconditioned gradient direction: $G_m = -\mathcal{P}\mathcal{G}(X_m)$; 6 Compute β_m according to the Polak-Ribière formula (other choices are equally possible) <div style="text-align: center; margin: 5px 0;"> $\beta_m = \frac{G_m^*(G_m - G_{m-1})}{G_{m-1}^* G_{m-1}};$ </div> 7 Update the conjugate direction $D_m = G_m + \beta_m G_{m-1}$; 8 Perform a line search in the direction of D_m and update X_{m+1}; 9 Set $m = m + 1$.
--

Algorithm 1: Preconditioned nonlinear conjugate gradient method.

The OMM method is highly efficient in each iteration, as involves only matrix-matrix multiplications that take $\mathcal{O}(nN^2 + Nn \log n)$ operations, where $n \log n$ comes from the FFT in the application of H (recall that a pseudospectral discretization is used). Hence, a good preconditioner for the OMM should be efficient to construct and simple to apply, so that it does not increase much the cost of each iteration; at the same time, we hope the preconditioner can reduce the number of iterations significantly.

2.2. Existing preconditioners. We shall first recall existing preconditioners for planewave discretization in general, which also apply for the OMM. The conventional preconditioning employed in the electronic structure calculation is in a form of inverse shifted Laplacian:

$$\mathcal{P} = P \otimes I_N, \quad \text{where, } P = (I - \tau^{-1} \Delta)^{-1}.$$

Here $-\Delta$ stands for the discretization of the Laplacian operator (kinetic energy operator in the Hamiltonian), and τ is a parameter setting the scale for the kinetic energy preconditioning. Note that in the planewave discretization, P is a diagonal matrix in the k -space

$$(5) \quad P_{kk'} = \delta_{kk'} (1 + \tau^{-1} |k|^2)^{-1},$$

and thus application of the preconditioner has minimal computational cost.

In practice, the preconditioner might take a more complicated expression (see e.g., the review article [23] and references therein)

$$(6) \quad P_{kk'} = \delta_{kk'} \frac{27 + 18s + 12s^2 + 8s^3}{27 + 18s + 12s^2 + 8s^3 + 16s^4}$$

with $s = |k|^2/\tau$ and τ a scaling parameter. This preconditioner was first proposed in [30] and is now known as the TPA preconditioner. It has a similar asymptotic behavior to (5) around $|k| = 0$ and as $|k| \rightarrow \infty$, but is found to be more efficient than (5) empirically.

A recent article [33] generalized the TPA preconditioner using polynomials with higher degrees than those in (6). More specifically, this new preconditioner, denoted as the generalized TPA preconditioner (gTPA), is based on a polynomial of degree t

$$p_t(s) := c_0 + c_1 s + c_2 s^2 + \dots + c_t s^t,$$

and takes the form

$$(7) \quad P_{kk'} = \delta_{kk'} \frac{p_t(s)}{p_t(s) + c_{t+1} s^{t+1}},$$

where $s = |k|^2/\tau$ as before. The polynomial p_t is constructed such that all the derivatives of $g_t(s) = \frac{p_t(s)}{p_t(s) + c_{t+1} s^{t+1}}$ up to order t at $s = 0$ vanish, meaning that the gTPA preconditioner is close to an identity operator in the low frequency regime and the width of this region depends on t . Note that, the TPA preconditioner is a special case of the gTPA preconditioners for $t = 3$ and the shifted Laplacian preconditioner in (5) is a special case of $t = 0$. From now on, P_t is used to denote the gTPA preconditioner corresponding to t . In the pseudospectral method, applying all the preconditioners above to a search direction only takes $\mathcal{O}(Nn \log n)$ operations since FFT is applied to N columns in the search direction $\mathcal{G}(X_m)$.

The physical intuition of all these preconditioners is that: 1) the preconditioner should keep the low-frequency components in the search direction unchanged; 2) g_t should have an asymptotic behavior like $\frac{1}{s}$ so that it behaves as an inverse Laplacian for the high-frequency components. Therefore, they act as a low-pass filter that is essentially similar to the inverse shifted Laplacian in 5. For the gTPA, as t increases, the low-frequency region is expanded while the high frequency components are further damped (see Figure 1 for an illustration).

As the behavior of these preconditioners is close to inverse shifted Laplacian, the success essentially lies in the assumption that the potential part of the Hamiltonian operator does not change the spectrum too much. When this assumption is not valid, these preconditioner might not be able to effectively reduce the condition number of the OMM.

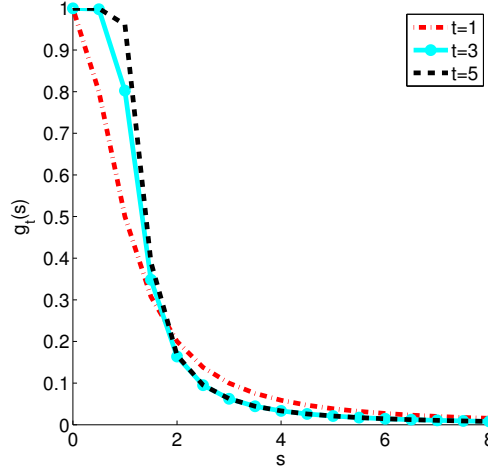


FIGURE 1. The function $g_t(x)$ in the gTPA preconditioner for $t = 1, 3$, and 5 .

2.3. Condition number of the preconditioned OMM. To understand the performance of the existing preconditioners in the context of OMM, we analyze here the condition number of the preconditioned OMM. While the condition number of the OMM (without preconditioning) was analyzed in [24], for completeness, we will also repeat the calculation here in a slightly different and more compact way.

Note that condition number of the TPA type preconditioning is rather complicated (if possible) to obtain analytically. For the purpose of simplicity, we consider a preconditioner of the type of inverse shifted Hamiltonian

$$(8) \quad P = (H - \mu I)^{-1},$$

which is more friendly for analysis (since it commutes with the Hamiltonian operator) and shares the same spirit with the TPA type preconditioners. In fact, as it takes into account both the kinetic and potential parts of the Hamiltonian, it captures better the spectral behavior of the Hamiltonian operator.

The Hessian of E_{omm} is given by

$$(9) \quad \mathcal{H}(X)Z = 2HZ - Z(X^*HX) - X(Z^*HX) - X(X^*HZ) - HZ(X^*X) - HX(Z^*X) - HX(X^*Z).$$

Let X_0 be the minimizer (i.e., the solution of the eigenvalue problem) such that $HX_0 = X_0\Lambda_0$, where Λ_0 is a diagonal matrix containing the eigenvalues. Evaluating the Hessian at the minimizer X_0 (orthonormalized such that $X_0^*X_0 = I_N$), we have

$$(10) \quad \mathcal{H}(X_0)Z = HZ - Z\Lambda_0 - X_0Z^*X_0\Lambda_0 - X_0\Lambda_0Z^*X_0 - 2X_0\Lambda_0X_0^*Z.$$

Note that the energy E_{omm} is invariant under any perturbation in the subspace of X_0 , we may assume that the perturbed direction is perpendicular, i.e., $Z^*X_0 = 0$. For such directions, we get

$$(11) \quad \mathcal{H}(X_0)Z = HZ - Z\Lambda_0.$$

Therefore, the condition number of \mathcal{H} is at least

$$(12) \quad \text{cond}(\mathcal{H}(X_0)) \geq \frac{\lambda_n - \lambda_1}{\lambda_{N+1} - \lambda_N},$$

determined by the ratio of the spectrum width of H and the spectral gap. In particular, this implies that if the gap between λ_N and λ_{N+1} is small relatively to the whole spectrum width of H , the condition number of the OMM minimization becomes large.

For the preconditioned gradient, we get

$$(13) \quad \mathcal{P}\mathcal{G}(X) = 2PHX - PX(X^*HX) - PHX(X^*X),$$

and thus

$$(14) \quad \mathcal{P}\mathcal{H}(X_0)Z = PHZ - PZ\Lambda_0.$$

The eigenvalues of the Hessian hence depend on $P(H - \lambda_i I)$, $i = 1, \dots, N$, and some of them take the form

$$(15) \quad 1 - \frac{\lambda_i - \mu}{\lambda_j - \mu}, \quad i \leq N < j.$$

To guarantee that the Hessian after preconditioning is positive definite, we consider the family of preconditioner with $P = (H - \mu I)^{-1}$ with $\mu < \lambda_{N+1}$. To estimate the condition number after preconditioning, we separate into several cases according to the position of μ in the spectrum of H .

- $\lambda_N < \mu < \lambda_{N+1}$, then the largest and the smallest eigenvalues of the form (15) after preconditioning are

$$\lambda_{\max} = 1 - \frac{\lambda_1 - \mu}{\lambda_{N+1} - \mu},$$

$$\lambda_{\min} = 1 - \frac{\lambda_N - \mu}{\lambda_n - \mu},$$

since $i \leq N$ and $N+1 \leq j$. Then the condition number is at least

$$(16) \quad \text{cond}(\mathcal{P}\mathcal{H}(X_0)) \geq \frac{1 - \frac{\lambda_1 - \mu}{\lambda_{N+1} - \mu}}{1 - \frac{\lambda_N - \mu}{\lambda_n - \mu}} = \frac{\lambda_{N+1} - \lambda_1}{\lambda_n - \lambda_N} \frac{\lambda_n - \mu}{\lambda_{N+1} - \mu}.$$

To minimize the condition number, we let $\mu \rightarrow \lambda_N$ and get

$$(17) \quad \text{cond}(\mathcal{P}\mathcal{H}(X_0)) \geq \frac{\lambda_{N+1} - \lambda_1}{\lambda_{N+1} - \lambda_N}.$$

- $\lambda_1 < \mu < \lambda_N$, then

$$\lambda_{\max} = 1 - \frac{\lambda_1 - \mu}{\lambda_{N+1} - \mu},$$

$$\lambda_{\min} = 1 - \frac{\lambda_N - \mu}{\lambda_{N+1} - \mu},$$

since $i \leq N$ and $N+1 \leq j$. Then the condition number is at least

$$(18) \quad \text{cond}(\mathcal{P}\mathcal{H}(X_0)) \geq \frac{1 - \frac{\lambda_1 - \mu}{\lambda_{N+1} - \mu}}{1 - \frac{\lambda_N - \mu}{\lambda_{N+1} - \mu}} = \frac{\lambda_{N+1} - \lambda_1}{\lambda_{N+1} - \lambda_N}.$$

- $\mu \leq \lambda_1$, then

$$(19) \quad \text{cond}(\mathcal{P}\mathcal{H}(X_0)) \geq \frac{1 - \frac{\lambda_1 - \mu}{\lambda_n - \mu}}{1 - \frac{\lambda_n - \mu}{\lambda_{N+1} - \mu}} = \frac{\lambda_n - \lambda_1}{\lambda_{N+1} - \lambda_N} \frac{\lambda_{N+1} - \mu}{\lambda_n - \mu}.$$

To minimize the condition number, we should take μ close to λ_1 in this case, which leads to

$$(20) \quad \text{cond}(\mathcal{P}\mathcal{H}(X_0)) \geq \frac{\lambda_{N+1} - \lambda_1}{\lambda_{N+1} - \lambda_N}.$$

Therefore, we arrive at the conclusion that the lower bound of the conditioner we can achieve by using a preconditioner of type $P = (H - \mu I)^{-1}$ with $\mu < \lambda_{N+1}$ is

$$\frac{\lambda_{N+1} - \lambda_1}{\lambda_{N+1} - \lambda_N}.$$

Hence, the condition number after preconditioning will still be large if the spectral gap between λ_N and λ_{N+1} is small.

The above conclusion can be understood by investigating the spectral meaning of an inverse shifted Hamiltonian of the form $(H - \mu I)^{-1}$, we see that this type of preconditioners prefers the eigenspace with eigenvalues close to the shift μ . This would limit the search direction in this spectral window and hence the OMM cannot converge to the right solution quickly, or even converges to an undesired solution. This motivates us to propose a new preconditioner based on an approximate Fermi operator projection that restricts the search direction in the full target eigenspace. This algorithm is presented in the next section.

3. ALGORITHM DESCRIPTION

The preconditioner we propose is based on the idea of using an approximate Fermi operator projection, as described in Section 3.1. The preconditioner has the form of a linear combination of shifted inverses of the Hamiltonian; so that to accelerate the construction and application, the sparsifying preconditioner [31] is used to iteratively solve the linear equation corresponds to the shifted inverse. The detail is given in Section 3.2. Last, it is possible to precompute and store the preconditioner in a data sparse format using rank revealing QR decomposition, as will be discussed in Section 3.3.

3.1. Fermi operator projection. In quantum mechanics, given an effective one-particle Hamiltonian H , the zero-temperature single-particle density matrix Π of the system is given by the Fermi operator via a Green's function expansion

$$(21) \quad \Pi = \frac{1}{2\pi i} \int_{\Gamma} (zI - H)^{-1} dz,$$

where Γ is a contour in the complex plane containing the N eigenvalues below the Fermi level. Note that by Cauchy's integral formula, Π defined in (21) is exactly the projection to the eigenspace corresponds to the first N eigenvalues. The contour integral representation of the Fermi operator has been a useful tool in electronic structure calculation, for example in linear scaling methods (see e.g., the review [8]). More recently, the contour integral formulation was used in the method of PEXSI [14–16] for a fast algorithm to obtain the density for sparse Hamiltonian matrices, combined with the selected inversion algorithm. It is also used in FEAST [26] as a general eigenvalue

solver for sparse Hamiltonian matrices. In [4], the contour integral was used for multishift problems. Our idea in this work is to explore the approximate Fermi operator projection as an effective preconditioner.

To use Π as an preconditioner, similar to what we did in [15], we employ the efficient quadrature rule proposed in [9] to discretize the contour integration (21) as

$$(22) \quad \Pi \approx \sum_{j=0}^p w_j (H - z_j I)^{-1}$$

where z_j is the j -th quadrature node on the contour and w_j is its corresponding weight. The above formula is also called pole expansion, as the quadrature points can be viewed as poles in the resolvents $(H - z_j I)^{-1}$ in the expansion. The approximation error of the quadrature rule is bounded by [15]

$$e^{-cp} \left(\log \frac{\lambda_n - \lambda_1}{\lambda_{N+1} - \lambda_N} + 3 \right)^{-1}.$$

The convergence of the quadrature rule is exponentially fast in p and hence only a small number of poles are needed. The details of the choice of w_j and z_j can be found in [15] and we will not repeat here.

We remark that if the projection is calculated by inverting $(H - z_j I)^{-1}$ exactly (or with a very small error tolerance), we get already the projection Π onto the low-lying eigenspace, i.e., the density matrix. Of course, direct inversion of $(H - z_j I)^{-1}$, for pseudospectral discretization, is equally expensive, since H is a dense matrix. This is different from the situation of PEXSI or FEAST where sparse Hamiltonian matrices are considered. An alternative approach to construct a precise projection is to use iterative matrix solvers to apply $(H - z_j I)^{-1}$. If a basis of the eigenspace is desired, it can be obtained by acting Π on a few vectors, as in the Fermi operator projection method [1, 8], or more systematically, by using a low-rank factorization via a randomized SVD [10]. However, to obtain high accuracy, this idea is still expensive since the matrix $(H - z_j I)$ is usually ill-conditioned and the iteration number might be large.

The key observation is that, as we plan to apply the projection as a preconditioner, we in fact do not really need the exact projection, as long as we can get a good approximation. Thus, it suffices to use an iterative scheme to solve $(H - z_j)^{-1}$ acting on some vector with a relatively large error tolerance. We aim to achieve a balance, such that the approximate projection is accurate enough such that the OMM converges in a few iterations, but also rough enough such that the construction is cheap.

More specifically, in the nonlinear conjugate gradient method for the OMM, the preconditioned gradient direction at the m -th step is computed by

$$(23) \quad G_m = -\mathcal{P}\mathcal{G}(X_m) = -\sum_{j=0}^p w_j Y_{m,j},$$

where $Y_{m,j} \in \mathbb{R}^{n \times N}$ is a rough solution of the linear system

$$(24) \quad (H - z_j I) Y_{m,j} = \mathcal{G}(X_m),$$

for $j = 1, \dots, p$. In the pseudospectral method, the matrix $H - z_j I$ can be applied efficiently via the FFT in $\mathcal{O}(n \log n)$ operations. Hence, the GMRES [29] with a large tolerance and a small number of maximum iterations is able to provide rough solutions to the linear systems in (24) quickly. Denote the number of iterations in GMRES by n_g , the total complexity for finding a

rough solution is $\mathcal{O}(pn_g N n \log n)$, which is of the same order as the complexity of the regular TPA and gTPA preconditioners. To further accelerate the GMRES iteration, the search direction $\mathcal{G}(X_m)$ is used as the initial guess for the GMRES, since it is almost in the eigenspace of interest if m is large. As we shall see later, the new preconditioner is highly efficient and the preconditioned OMM will converge in only a few iterations.

3.2. Sparsifying preconditioner. In the previous subsection, an approximate Fermi operator projection is introduced as a preconditioner for the OMM. As we shall see later in the numerical section, the preconditioned OMM converges quickly in a few iterations. Hence, the difficulty of solving an eigenvalue problem with the OMM has been replaced by the difficulty of constructing the projection efficiently, the most expensive part of which is solving linear systems with multiple right-hand sides. Since these linear systems are solved roughly in an iterative scheme like the GMRES, the preconditioning problem for the OMM is transferred to the preconditioning problem for the GMRES.

In the case when the Hamiltonian operator $H = -\frac{1}{2}\Delta + V - \mu$ behaves like a kinetic energy operator, i.e., the potential energy operator is negligible, a conventional preconditioner for the linear system

$$(25) \quad (H - \mu I)u = b$$

is

$$P = \left(-\frac{1}{2}\Delta - s\right)^{-1},$$

where s is a proper shift. However, when the contribution of the potential energy operator V is large, e.g., in highly indefinite systems on periodic structures, an inverse shifted Laplacian is no longer an efficient preconditioner, e.g., the GMRES might take a very large number of iterations to converge or it even diverges. To overcome this difficulty, we will adopt the recently proposed sparsifying preconditioner for solving the linear systems in the construction of the approximate Fermi operator projection.

Let us focus on the numerical solution of (25). We assume that the computation domain is the periodic unit box $[0, 1]^d$ and discretize the problem using the Fourier pseudospectral method. With abuse of notations, the discretized problem of (25) takes the form

$$(26) \quad \left(-\frac{1}{2}\Delta + V - \mu\right)u = b.$$

We will briefly recall the key idea of the sparsifying preconditioner for solving this type of equations. More details can be found in [31] (see also [17, 32]).

Denote $l = \langle V \rangle$ the spatial average of V . We assume without loss of generality that $-\frac{1}{2}\Delta + l - \mu$ is invertible on \mathbb{T}^d with periodic boundary condition, otherwise, we will use a slight perturbation of μ instead and put the difference into V . This allows us to rewrite (25) trivially as

$$(27) \quad \left(-\frac{1}{2}\Delta + (l - \mu) + (V - l)\right)u = b$$

Applying the Green's function of the constant part $G = \left(-\frac{1}{2}\Delta + (l - \mu)\right)^{-1}$ via the FFT to both sides of (25), we have an equivalent linear system

$$(28) \quad (I + G(V - l))u = Gb.$$

The main idea of the sparsifying preconditioner is to multiply a particular sparse matrix Q (to be defined later) on the both hand sides of (28):

$$(29) \quad (Q + QG(V - l))u = Q(Gb),$$

so to make the matrix on the left hand in (29) becomes sparse. To see how this is possible, let $S = \{(j, a(j)), j \in J\}$ be the support of the sparse matrix Q , i.e., for each point j , the row $Q(j, :)$ is supported in a local neighborhood $a(j)$. If for each point j , the Q is constructed such that

$$(QG)(j, a(j)^c) = Q(j, a(j))G(a(j), a(j)^c) \approx 0,$$

then the product QG is also essentially supported on S . The sum $Q + QG(V - l)$ is essentially supported in S as well, since $(V - l)$ is a diagonal matrix. The above requirement can indeed be achieved since G , after all, is the Green's function of a local operator; thus Q is a discrete approximation of the differential operator. More details can be found in [31].

Restricting $Q + QG(V - l)$ to S by thresholding other values to zero, we define a sparse matrix P

$$(30) \quad P_{ij} = \begin{cases} (Q + QG(V - l))_{ij}, & (i, j) \in S, \\ 0, & (i, j) \notin S. \end{cases}$$

Since $P \approx Q + QG(V - l)$, we have the approximate equation

$$(31) \quad Pu \approx Q(Gb).$$

The sparsifying preconditioner computes an approximate solution \tilde{u} by solving

$$P\tilde{u} = Q(Gb).$$

Since P is sparse, the above equation can be solved by sparse direct solvers such as the nested dissection algorithm [6]. The solution $\tilde{u} = P^{-1}QGb$ can be used as a preconditioner for the standard iterative algorithms such as GMRES [29] for the solution of (26).

In the construction of the sparsifying preconditioner, the most expensive part is to build the nested dissection factorization for P , the complexity of which scales as $\mathcal{O}(n^{1.5})$ in two dimensions and $\mathcal{O}(n^2)$ in three dimensions. The application of the sparsifying preconditioner is very efficient and takes only $\mathcal{O}(n \log n)$ operations in two dimensions and $\mathcal{O}(n^{4/3})$ operations in three dimensions. Since the dominant cost of the OMM with pseudospectral discretization is $\mathcal{O}(nN^2)$, where N is proportional to n , the construction and the application of the sparsifying preconditioner is relatively cheap for large-scale problems. As we shall see in the numerical section, even if n is as small as 576, the preconditioned OMM with the sparsifying preconditioner is still more efficient than the one with a regular preconditioner.

3.3. Precomputing the preconditioner. When the problem size n is not sufficiently large, the prefactor pn_g in the application complexity of the approximate projection might be too large. It is better to use a randomized low-rank factorization method to construct a matrix representation UU^* of the preconditioner such that

$$UU^*b \approx \sum_{j=0}^p w_j (H - z_j I)^{-1} b,$$

for an arbitrary vector $b \in \mathbb{R}^n$, where $U \in \mathbb{C}^{n \times N}$ is a unitary matrix (and hence the notation U). Therefore, UU^* is a data-sparse way to store the matrix preconditioner. Adapting the randomized SVD method [10], a fast algorithm for constructing the matrix U is given below.

- 1 Given the Hamiltonian H and the range of the eigenvalues, construct the quadrature nodes and weights $\{z_j, w; j\}_{1 \leq j \leq p}$ for the contour integration in 21;
- 2 Construct a Gaussian random matrix $B \in \mathbb{R}^{n \times (N+k)}$, where k is a non-negative constant integer;
- 3 Solve the linear systems $(H - z_j I)Y_j = B$ for each $j = 1, \dots, p$ using the GMRES with the right-hand side as the initial guess.
- 4 Compute $Y = \sum_{j=0}^p w_j Y_j$;
- 5 Apply a rank-revealing QR factorization $[U, R] = \text{qr}(Y)$;
- 6 Update U by selecting the first N columns: $U = U(:, 1 : N)$;
- 7 The approximate Fermi operator projection is given by UU^* .

Algorithm 2: Randomized low-rank factorization for the Fermi operator projection.

The operation complexity of Algorithm 2 is $\mathcal{O}(pn_g N n \log n + nN^2)$, where nN^2 comes from the QR factorization. When N is very large and nN^2 dominates the construction complexity of the preconditioner, it is better to apply the projection in (23) directly without the QR factorization, while for smaller scale problems, the pre-computation accelerates the overall calculation.

We remark that the scalability of the rank-revealing QR factorization in high performance computing has been an active research direction, see for example the communication-reduced QR factorization recently proposed in [18] and implemented in Elemental [28]. Due to the large prefactor of the complexity of the communication-reduced QR factorization, applying it for many times is still quite expensive. This makes Algorithm 2 better than those with QR factorization in each iteration, e.g., in conventional ways to solve for 1. Parallelism of other steps is straightforward: 1) each linear system at each pole z_j can be solved simultaneously; 2) parallel GMRES routines have been standard in high performance computing; 3) applying this approximate Fermi operator projection is simple matrix-matrix multiplication with complexity $\mathcal{O}(nN^2)$.

4. NUMERICAL EXAMPLES

This section presents numerical results to support the efficiency of the proposed algorithm. Numerical results were obtained in MATLAB on a Linux computer with CPU speed at 3.5GHz. The number of poles in the contour integration was 30. The GMRES algorithm in the construction of the approximate Fermi operator projection was used with a relative tolerance equal to 10^{-5} , a restart number equal to 15, and a maximum iteration number equal to 5 (i.e., the total maximum iterations allowed in the GMRES is 75). In the randomized algorithm for constructing a matrix representation UU^* of the approximate Fermi operator projection, a random Gaussian matrix B of size $n \times N$ was used. In the OMM, the convergence tolerance was 10^{-13} and the maximum iteration number is 4000.

Numerical experiments corresponding to three different kinds of Hamiltonian operators in two dimensions are presented: 1) the potential energy is much weaker than the kinetic energy, i.e., the kinetic energy operator dominates the Hamiltonian operator; 2) the potential energy is prominent, contains one defect, and the Hamiltonian operator behaves different from the kinetic operator; 3) the potential energy is more prominent and contains more defects, so that the

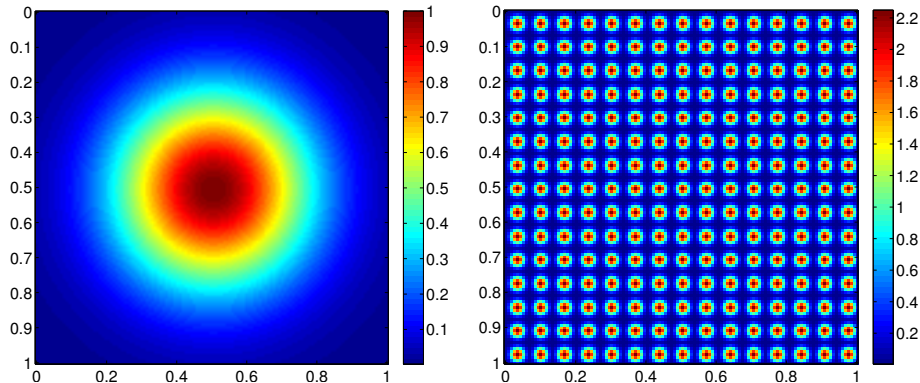


FIGURE 2. Left: the periodic function $V_0(\mathbf{r})$ is a Gaussian well on the unit square $[0, 1]^2$. Right: the potential energy operator $\ell^2 V(\ell \mathbf{x})$ on the unit square $[0, 1]^2$ after scaling with $\ell = 15$ in Test 1.

Hamiltonian operator behaves further different from the kinetic operator. These experiments demonstrate that the proposed preconditioner has better performance than the regular preconditioners in a wide range of circumstances.

In our numerical tests, the contour construction is based on the exact spectral information of the H . The starting guess for the conjugate gradient procedure in the OMM is generated by diagonalizing the Hamiltonian H , selecting the low-lying eigenpairs, and adding Gaussian random noise with a distribution $\mathcal{N}(0, 0.1M^2)$ to the eigenvectors, where M is the maximum magnitude of the ground truth eigenvectors. Since the proposed preconditioner is also an approximate spectral projector onto the desired eigen subspace, we applied it to filter the initial guess before the preconditioned conjugate gradient scheme. In practice, spectral information can be estimated in the previous step of the self-consistent field iteration in electronic structure calculation.

4.1. Test 1. In the first test, the Hamiltonian matrix H is a discrete representation of the Hamiltonian operator in two dimensions

$$(32) \quad \left(-\frac{\Delta}{2} + V(\mathbf{r}) \right) \phi_j(\mathbf{r}) = \epsilon_j \phi_j(\mathbf{r}), \quad \mathbf{r} \in \ell \mathbb{T}^2 := [0, \ell]^2,$$

with a periodic boundary condition, where $V(\mathbf{r})$ is the potential field, ϵ_j is the orbital energy of the corresponding Kohn-Sham orbital, $\phi_j(\mathbf{r})$. It is convenient to rescale the system to the unit square via the transformation $\ell \mathbf{x} = \mathbf{r}$:

$$(33) \quad \left(-\frac{\Delta}{2} + \ell^2 V(\ell \mathbf{x}) \right) \phi_j(\mathbf{x}) = \epsilon_j \ell^2 \phi_j(\mathbf{x}), \quad \mathbf{x} \in \mathbb{T}^2 := [0, 1]^2,$$

and discretize the new system with the pseudospectral method. Define

$$J = \{(j_1, j_2) \mid 0 \leq j_1, j_2 < \sqrt{n}\},$$

$$K = \{(k_1, k_2) \mid -\sqrt{n}/2 \leq k_1, k_2 < \sqrt{n}/2\}.$$

Suppose F and F^{-1} are the discrete Fourier and inverse Fourier transforms. After discretization, the corresponding eigenvalue problem of Equation (33) becomes

$$(34) \quad HX = X\Lambda$$

in numerical linear algebra, where $H = -\frac{\Delta}{2} + V$,

$$-\frac{\Delta}{2} = F^{-1} \text{diag}(2\pi^2 |k|^2)_{k \in KF},$$

and

$$V = \ell^2 \text{diag} \left(V \left(\frac{\ell j}{\sqrt{n}} \right) \right)_{j \in J},$$

Λ is a diagonal matrix containing eigenvalues, and X contains the eigenvectors.

Let $V_0(\mathbf{r})$ be a Gaussian well on the unit square $[0, 1)^2$ (see Figure 2 left panel) and extend it periodically with period 1 in both dimensions. In the first test, the potential term $V(\mathbf{r})$ (see Figure 2 right panel) in (33) is chosen to be $0.01 V_0(\mathbf{r})$ so that the kinetic energy operator $-\frac{\Delta}{2}$ dominates the Hamiltonian operator. Hence, the spectrum of H is very close to the one of $-\frac{\Delta}{2}$. The preconditioned OMM is applied to solve the eigenvalue problem in (34). The numerical performance of the empirical preconditioner in (6) (denoted as TPA) and its generalization in (7) when $t = 5$ (denoted as gTPA), and the new preconditioner via an approximate Fermi operator projection (denoted as SPP or PP with or without the sparsifying preconditioner, respectively), is compared and summarized in Table 1 and Figure 3. The scaling parameter τ in the TPA and gTPA preconditioner takes the value $\max_j \sum_k \frac{1}{2} |k|^2 (x^{(j)}(k))^2$, where $x^{(j)}$ is the j th column of ground true eigenspace FX_0 and k is the two-dimensional index in K . For each Hamiltonian H with a fixed ℓ , 5 experiments were repeated with different random initial guesses. In this summary, some notations are introduced and recalled as follows:

- n is the dimension of H ;
- ℓ is the number of cells in the domain of $V(\mathbf{r})$ and each cell $[0, 1)^2$ contains a grid of size 8×8 ; $N = \ell$;
- cond is the condition number of the OMM;
- iter is the number of iterations in the preconditioned OMM;
- T_{st} is the setup time of the preconditioner; for PP and SPP, T_{st} is the setup time per pole.
- T_{omm} is the running time of the preconditioned OMM;
- $T_{\text{tot}} = T_{\text{st}} + T_{\text{omm}}$;
- d measures the distance between the column space of the ground truth eigenvectors X_0 and the one of the estimated eigenvectors X by the preconditioned OMM:

$$d(X, X_0) = \frac{\|X(X^*X)^{-1}X^* - X_0(X_0^*X_0)^{-1}X_0^*\|}{\|X_0(X_0^*X_0)^{-1}X_0^*\|},$$

where the norm here is the entrywise ℓ^∞ norm.

The preconditioner TPA and gTPA essentially assume that the potential $V(\mathbf{r})$ is negligible and they can be implemented efficiently using the fast Fourier transform. Hence, they would be efficient in the numerical examples in Test 1 and this is supported by the results below: T_{st} is negligible; the preconditioned OMM converges in a few hundred iterations; the OMM returns an eigenspace close to the ground truth, i.e., the measurement d is almost 0.

	(ℓ, n)	cond	iter	$T_{st}(sec)$	$T_{omm}(sec)$	$T_{tot}(sec)$	d
TPA	(3,576)	1.4e+02	5.8e+02	2.271e-03	1.669e+00	1.672e+00	9.0e-07
gTPA	(3,576)	1.4e+02	5.6e+02	2.067e-03	1.695e+00	1.697e+00	7.8e-07
PP	(3,576)	1.4e+02	3.0e+00	1.486e-02	1.063e-02	2.549e-02	4.4e-10
TPA	(5,1600)	8.0e+02	7.4e+02	4.380e-04	6.821e+00	6.822e+00	7.5e-06
gTPA	(5,1600)	8.0e+02	6.2e+02	5.310e-04	5.801e+00	5.802e+00	6.6e-06
PP	(5,1600)	8.0e+02	3.0e+00	4.204e-02	3.483e-02	7.686e-02	1.6e-10
TPA	(7,3136)	1.6e+03	7.7e+02	1.596e-03	2.387e+01	2.388e+01	1.0e-05
gTPA	(7,3136)	1.6e+03	5.1e+02	2.333e-03	1.672e+01	1.673e+01	1.1e-05
PP	(7,3136)	1.6e+03	3.0e+00	1.464e-01	1.249e-01	2.713e-01	2.5e-10
TPA	(11,7744)	1.3e+03	6.6e+02	4.097e-03	1.417e+02	1.417e+02	8.8e-06
gTPA	(11,7744)	1.3e+03	5.0e+02	4.640e-03	1.086e+02	1.086e+02	7.5e-06
PP	(11,7744)	1.3e+03	3.0e+00	6.151e-01	7.096e-01	1.325e+00	4.5e-10
TPA	(15,14400)	7.2e+03	7.2e+02	1.296e-02	6.263e+02	6.263e+02	1.1e-05
gTPA	(15,14400)	7.2e+03	6.0e+02	1.245e-02	5.120e+02	5.121e+02	1.1e-05
PP	(15,14400)	7.2e+03	4.0e+00	1.622e+00	3.997e+00	5.619e+00	8.9e-10
TPA	(23,33856)	1.7e+04	1.1e+03	6.347e-02	7.920e+03	7.920e+03	1.1e-05
gTPA	(23,33856)	1.7e+04	5.1e+02	6.488e-02	3.727e+03	3.727e+03	1.2e-05
PP	(23,33856)	1.7e+04	3.0e+00	9.595e+00	2.531e+01	3.490e+01	3.3e-09

TABLE 1. Numerical results in Test 1 when $V(\mathbf{r}) = 0.01V_0(\mathbf{r})$.

Even in this case which favors the conventional preconditioners, the new preconditioner via an approximate Fermi operator projection (PP) is much more efficient. Even though the approximation accuracy of the Fermi operator projection is low, since the tolerance of the GMRES in computing the contour integration is large, this rough projection as a preconditioner is able to reduce the iteration number of the OMM to 3 or 4 in all examples. The total running time of PP, including the setup time of the preconditioner and the running time of the OMM, is far less than those of TPA and gTPA. The speedup factor is significant and increases as the problem gets larger in most cases as show in Figure 3. The measurement d is much smaller than those in the TPA and gTPA methods, which means that the solution of the OMM is more accurate than the TPA and gTPA methods. We remark that the solutions for linear systems at different poles can be straightforwardly parallelized, here we only use the setup time per pole in the comparison and focus on the time spent on the iterative procedures of GMRES and OMM that can not be parallelized. Since the GMRES with a regular preconditioner is already rather efficient and the iteration converges less than 5 iterations, the sparsifying preconditioner is not applied in Test 1.

4.2. Test 2. In the second test, the Hamiltonian matrix H is a discrete representation of the Hamiltonian operator in a two-dimensional Kohn-Sham equation similar to the one in (32), but the potential energy operator is more prominent and has a local defect representing a vacancy of the lattice, i.e., there is a random vacant cell in $[0, \ell]^2$. The potential energy operator $V(\mathbf{r})$ is

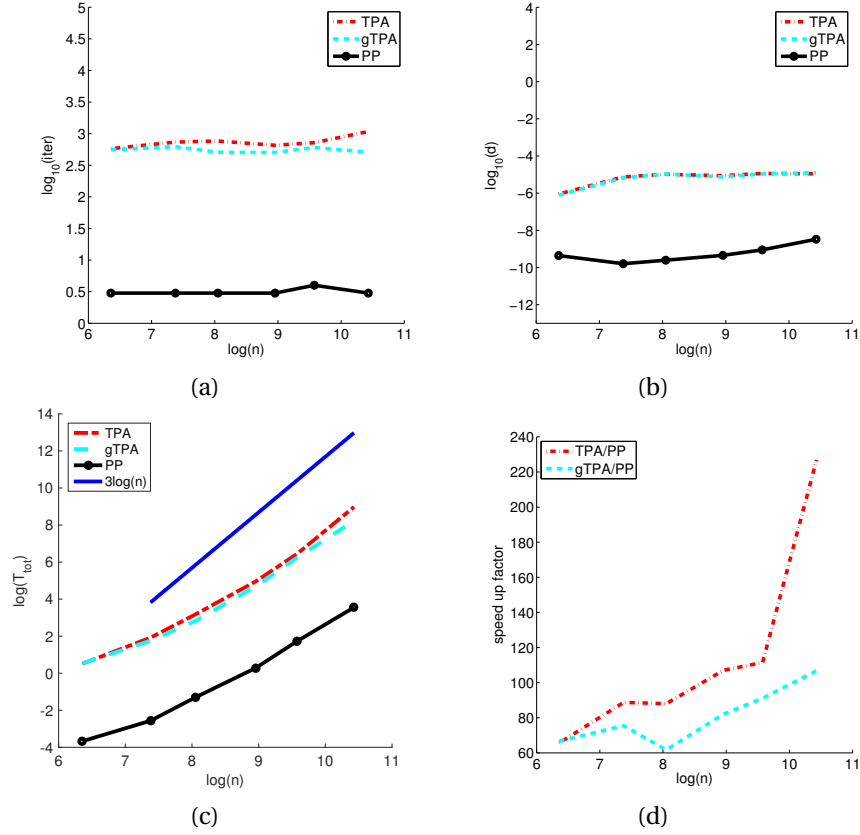


FIGURE 3. Numerical results in Test 1 when $V(\mathbf{r}) = 0.01V_0(\mathbf{r})$. (a) the number of iterations in the preconditioned OMM. (b) the measurement $d(X, X_0)$. (c) the total running time T_{tot} . (d) the speedup factor of the PP method compared with the TPA and gTPA method.

constructed by randomly covering a Gaussian well in $V_0(\mathbf{r})$ with a zero patch (see Figure 4 left panel for an example).

The Hamiltonian matrix H is not dominated by the kinetic matrix $-\frac{\Delta}{2}$ and hence their spectra are different. Therefore, the performance of the regular preconditioners TPA and gTPA in Test 2 might not be as good as in Test 1. For a similar problem size n , the number of iterations in the OMM is significantly larger than the one in Test 1. The measurement $d(X, X_0)$ is as large as $1e-4$ meaning that the preconditioned OMM with TPA and gTPA becomes less accurate in revealing the true eigenspace. Since the number of vacant cells is fixed, the influence of the local defect becomes weaker as the number of cells ℓ (per dimension) becomes larger. Hence, the Hamiltonian H becomes closer to the kinetic operator and the number of iteration decreases. This also shows that the performance of TPA and gTPA is better for Hamiltonian matrices close to the kinetic part.

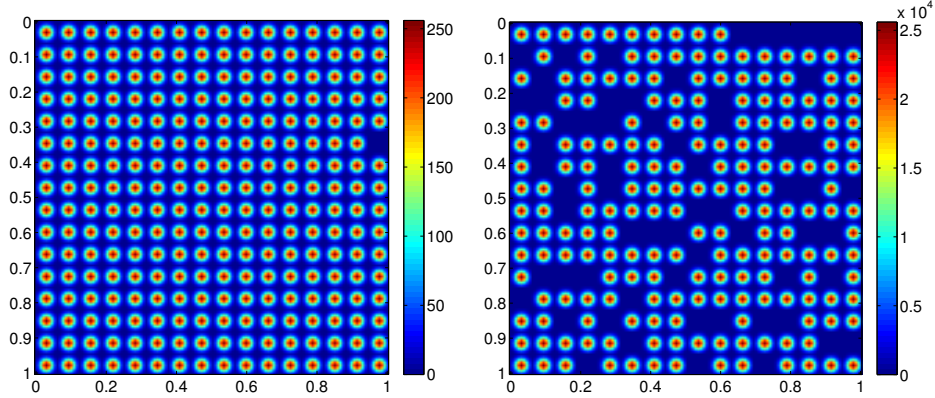


FIGURE 4. Left: the potential energy operator $V(\mathbf{r})$ with $\ell = 16$ in Test 2. Right: the potential energy operator $V(\mathbf{r})$ with $\ell = 16$ in Test 3.

In Test 2, since the potential energy is prominent and the Hamiltonian operator behaves far from the kinetic operator, the GMRES with an inverse shifted kinetic energy operator is not efficient for solving linear systems like

$$(H - z_k I)x = b.$$

The GMRES and the recently developed sparsifying preconditioner [17, 31, 32] are applied to solve the above system in Test 2 and 3. The preconditioner via an approximate Fermi operator projection for the OMM is hence denoted as SPP. As shown in Table 2 and Figure 5, the performance of the SPP method is better than the TPA and gTPA methods: the number of iteration in the OMM is a small number of $\mathcal{O}(1)$; the preconditioned OMM with SPP is able to provide an eigenspace closer to the ground truth; the SPP method is much faster and the speedup factor tends to increase with n .

4.3. Test 3. In the last test, the potential energy operator in Test 2 is multiplied by 100 and 25% of the cells are randomly covered by zero patches (see Figure 4 right panel for an example). Different from Test 2 that keeps the same number of vacant cells and varies the problem size, the number of vacant cells in Test 3 is proportional to the problem size so that the Hamiltonian matrix H stays far away from the kinetic matrix $-\frac{\Delta}{2}$, and their spectra are very different. Hence, the preconditioned OMM with TPA or gTPA is no longer efficient for all problem sizes.

As shown in Table 3 and Figure 6, the preconditioned OMM with TPA or gTPA requires thousands of iterations to converge or cannot converge within the maximum number of iteration, 4000. Even if the OMM converges, it cannot return useful estimation of the eigenspace, since the measurement $d(X, X_0)$ is too large.

In contrast, the OMM with SPP is still able to provide reasonably good estimation of the eigenspace within $\mathcal{O}(1)$ iterations. Although the iteration number increases with the system size n , it remains quite small even for large-scale problems.

	(ℓ, n)	cond	iter	$T_{st}(sec)$	$T_{omm}(sec)$	$T_{tot}(sec)$	d
TPA	(2,256)	3.7e+03	1.7e+03	5.514e-04	2.295e+00	2.296e+00	5.0e-05
gTPA	(2,256)	3.7e+03	1.1e+03	5.518e-04	1.423e+00	1.423e+00	4.1e-05
SPP	(2,256)	3.7e+03	3.0e+00	4.175e-02	4.708e-03	4.646e-02	3.1e-10
TPA	(4,1024)	2.4e+05	1.3e+03	2.652e-04	7.180e+00	7.180e+00	8.5e-05
gTPA	(4,1024)	2.4e+05	9.2e+02	3.680e-04	5.052e+00	5.053e+00	8.5e-05
SPP	(4,1024)	2.4e+05	3.0e+00	2.074e-01	2.007e-02	2.275e-01	2.1e-09
TPA	(8,4096)	9.4e+05	6.9e+02	1.098e-03	3.542e+01	3.542e+01	2.5e-05
gTPA	(8,4096)	9.4e+05	5.2e+02	1.489e-03	2.680e+01	2.680e+01	2.5e-05
SPP	(8,4096)	9.4e+05	3.0e+00	2.590e+00	1.965e-01	2.787e+00	1.8e-08
TPA	(16,16384)	7.4e+05	8.3e+02	1.432e-02	1.096e+03	1.096e+03	1.8e-05
gTPA	(16,16384)	7.4e+05	6.6e+02	1.453e-02	8.630e+02	8.630e+02	1.8e-05
SPP	(16,16384)	7.4e+05	3.0e+00	3.774e+01	5.000e+00	4.274e+01	3.8e-08
TPA	(32,65536)	3.1e+06	8.1e+02	1.754e-01	3.211e+04	3.211e+04	1.5e-05
gTPA	(32,65536)	3.1e+06	5.7e+02	2.054e-01	2.251e+04	2.251e+04	1.5e-05
SPP	(32,65536)	3.1e+06	3.0e+00	6.459e+02	1.473e+02	7.932e+02	1.5e-07

TABLE 2. Numerical results in Test 2.

	(ℓ, n)	cond	iter	$T_{st}(sec)$	$T_{omm}(sec)$	$T_{tot}(sec)$	d
TPA	(2,256)	6.8e+02	6.4e+02	1.098e-03	2.602e+00	2.603e+00	7.4e-06
gTPA	(2,256)	6.8e+02	5.5e+02	9.694e-04	2.244e+00	2.245e+00	7.0e-06
SPP	(2,256)	6.8e+02	3.0e+00	9.940e-02	8.341e-03	1.077e-01	2.7e-10
TPA	(4,1024)	2.5e+03	7.5e+02	6.446e-04	7.374e+00	7.374e+00	3.9e-05
gTPA	(4,1024)	2.5e+03	6.5e+02	4.654e-04	6.401e+00	6.402e+00	3.8e-05
SPP	(4,1024)	2.5e+03	4.0e+00	6.153e-01	6.153e-02	6.768e-01	1.2e-10
TPA	(8,4096)	3.7e+03	2.0e+03	2.367e-03	1.562e+02	1.562e+02	4.9e-05
gTPA	(8,4096)	3.7e+03	1.5e+03	2.307e-03	1.151e+02	1.151e+02	5.4e-05
SPP	(8,4096)	3.7e+03	4.0e+00	8.540e+00	4.380e-01	8.978e+00	5.2e-10
TPA	(16,16384)	2.4e+04	3.0e+03	2.196e-02	5.557e+03	5.557e+03	1.1e-04
gTPA	(16,16384)	2.4e+04	3.0e+03	2.476e-02	5.509e+03	5.509e+03	7.8e-05
SPP	(16,16384)	2.4e+04	7.0e+00	1.288e+02	1.563e+01	1.444e+02	1.1e-09
TPA	(32,65536)	1.4e+05	-	2.016e-01	1.595e+05	1.595e+05	8.7e-04
gTPA	(32,65536)	1.4e+05	-	2.308e-01	1.593e+05	1.593e+05	6.0e-04
SPP	(32,65536)	1.4e+05	1.5e+01	1.578e+03	6.779e+02	2.256e+03	2.8e-07

TABLE 3. Numerical results in Test 3. “-” means exceeding the maximum iteration number 4000.

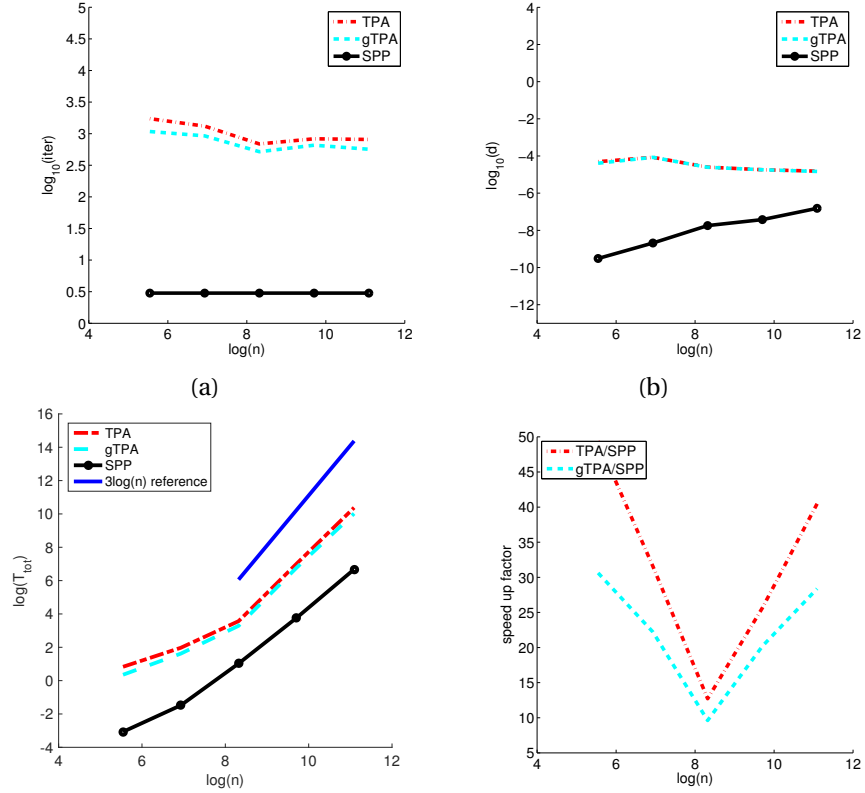


FIGURE 5. Numerical results in Test 2. (a) the number of iterations in the preconditioned OMM. (b) the measurement $d(X, X_0)$. (c) the total running time T_{tot} . (d) the speedup factor of the PP method compared with the TPA and gTPA method.

5. CONCLUSION AND REMARKS

This paper presents a novel preconditioner for the orbital minimization method (OMM) from planewave discretization. Once constructed, the application of the preconditioner is very efficient and the preconditioned OMM converges in $\mathcal{O}(1)$ iterations. Based on the approximate Fermi operator projection, this preconditioner can be constructed efficiently via iterative matrix solvers like GMRES with the newly developed sparsifying preconditioner. The speedup factor of the running time compared with existing preconditioned OMMs is as large as hundreds of times and the speedup factor tends to increase with the problem size. Numerical experiments also show that the new preconditioned OMM is able to provide more accurate solutions than the popular TPA preconditioner and, as a result, might reduce the number of iterations in the self-consistent field iteration.

This preconditioner based on spectral projection can be considered for other discretization schemes using localized basis functions, e.g., numerical atomic orbitals and wavelets that lead to sparse Hamiltonians. In these cases, sparse direct solvers or preconditioned iterative solvers

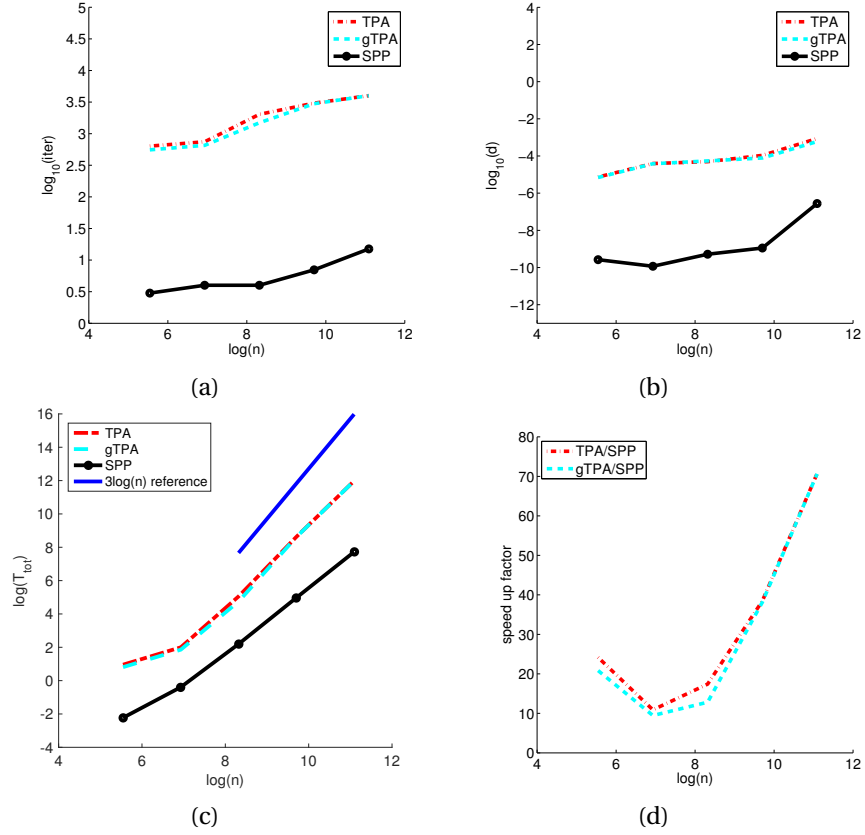


FIGURE 6. Numerical results in Test 3. (a) the number of iterations in the preconditioned OMM. (b) the measurement $d(X, X_0)$. (c) the total running time T_{tot} . (d) the speedup factor of the PP method compared with the TPA and gTPA method.

could be applied to construct the approximate Fermi operator projection via the pole expansion. This would be worth exploring as future directions.

It would be also of interest to implement our new algorithm into the recently developed parallel library for the OMM framework, libomm [3] and incorporate into existing electronic structure software packages. Parallelism of this new preconditioned OMM is straightforward since the main routines of this algorithm have parallel analog in existing high performance computing packages. Several versions of parallel FFT can be found in [25, 27]; the computational cost per processor is less in the former one, while the latter one has a better scalability and the number of processor can be $\mathcal{O}(n)$; a recent article [13] reduces the prefactor of the algorithm in [27] to an optimal one in the butterfly scheme while keeping the same scalability. The pole expansion can be embarrassingly parallelized. The last main routine, if applied, is the scalable QR factorization used for precomputing and storing the preconditioner in a data-sparse format. This has been implemented in Elemental [28]. For plane wave discretization, a recent article [12] has shown

that the constrained minimization model in (1) with a Chebyshev filter [34] outperforms the locally optimal block preconditioned conjugate gradient (LOBPCG) algorithm [11], implemented in ABINIT [2], in terms of scalability, even though a direct diagonalization of a matrix of size $N \times N$ is required in the Chebyshev filter in each iteration. Since the new preconditioned OMM requires no direct diagonalization, it is promising to lead to a more scalable approach.

REFERENCES

- [1] S. Baroni and P. Giannozzi, *Towards very large-scale electronic-structure calculations*, Europhys. Lett. **17** (1992), 547–552.
- [2] F. Bottin, S. Leroux, A. Knyazev, and G. Zérah, *Large-scale ab initio calculations based on three levels of parallelization*, Comput. Mater. Sci. **42** (2008), no. 2, 329–336.
- [3] E. Corsetti, *The orbital minimization method for electronic structure calculations with finite-range atomic basis sets*, Comput. Phys. Commun. **185** (2014), 873–883.
- [4] A. Damle, L. Lin, and L. Ying, *Pole expansion for solving a type of parametrized linear systems in electronic structure calculations*, SIAM J. Sci. Comput. **36** (2014), no. 6, A2929–A2951.
- [5] J. W. Demmel, L. Grigori, M. Gu, and H. Xiang, *Communication avoiding rank revealing QR factorization with column pivoting*, SIAM J. Matrix Anal. Appl. **36** (2015), no. 1, 55–89.
- [6] A. George, *Nested dissection of a regular finite element mesh*, SIAM J. Numer. Anal. **10** (1973), 345–363.
- [7] S. Goedecker, *Low complexity algorithms for electronic structure calculations*, J. Comput. Phys. **118** (1995), no. 2, 261–268.
- [8] S. Goedecker, *Linear scaling electronic structure methods*, Rev. Mod. Phys. **71** (1999), 1085–1123.
- [9] N. Hale, N. J. Higham, and L. N. Trefethen, *Computing a^α , $\log(a)$, and related matrix functions by contour integrals*, SIAM J. Numer. Anal. **46** (2008), no. 5, 2505–2523.
- [10] N. Halko, P. G. Martinsson, and J. A. Tropp, *Finding structure with randomness: Probabilistic algorithms for constructing approximate matrix decompositions*, SIAM review **53** (2011), no. 2, 217–288.
- [11] A. V. Knyazev, *Toward the optimal preconditioned eigensolver: Locally optimal block preconditioned conjugate gradient method*, SIAM J. Sci. Comput. **23** (2001), no. 2, 517–541.
- [12] A. Levitt and M. Torrent, *Parallel eigensolvers in plane-wave density functional theory*, Comput. Phys. Commun. **187** (2015), 98–105.
- [13] Y. Li and H. Yang, *Interpolative butterfly factorization*, 2016. preprint.
- [14] L. Lin, J. Lu, L. Ying, R. Car, and W. E, *Fast algorithm for extracting the diagonal of the inverse matrix with application to the electronic structure analysis of metallic systems*, Comm. Math. Sci. **7** (2009), 755–777.
- [15] L. Lin, J. Lu, L. Ying, and W. E, *Pole-based approximation of the Fermi-Dirac function*, Chin. Ann. Math. Ser. B **30** (2009), no. 6, 729–742.
- [16] L. Lin, C. Yang, J. Lu, L. Ying, and W. E, *A fast parallel algorithm for selected inversion of structured sparse matrices with application to 2d electronic structure calculations*, SIAM J. Sci. Comput. **33** (2011), no. 3, 1329–1351.
- [17] J. Lu and L. Ying, *Sparsifying preconditioner for soliton calculations*, J. Comput. Phys. in press.
- [18] P. G. Martinsson, *Blocked rank-revealing QR factorizations: How randomized sampling can be used to avoid single-vector pivoting*, 2015. preprint.
- [19] F. Mauri and G. Galli, *Electronic structure calculations and molecular dynamics simulations with linear system-size scaling*, Phys. Rev. B **50** (1994), 4316–4326.
- [20] F. Mauri, G. Galli, and R. Car, *Orbital formulation for electronic-structure calculations with linear system-size scaling*, Phys. Rev. B **47** (1993), 9973–9976.
- [21] P. Ordejón, D. A. Drabold, M. P. Grumbach, and R. M. Martin, *Unconstrained minimization approach for electronic computations that scales linearly with system size*, Phys. Rev. B **48** (1993), 14646–14649.
- [22] P. Ordejón, D. A. Drabold, R. M. Martin, and M. P. Grumbach, *Linear system-size scaling methods for electronic-structure calculations*, Phys. Rev. B **51** (1995), 1456–1476.
- [23] M.C. Payne, M.P. Teter, D.C. Allan, T.A. Arias, and J.D. Joannopoulos, *Iterative minimization techniques for ab initio total-energy calculations: molecular dynamics and conjugate gradients*, Rev. Mod. Phys. **64** (1992), 1045–1097.
- [24] B. G. Pfrommer, J. Demmel, and H. Simon, *Unconstrained energy functionals for electronic structure calculations*, J. Comput. Phys. **150** (1999), 287–298.

- [25] M. Pippig, *PFFT: An extension of FFTW to massively parallel architectures*, SIAM J. Sci. Comput. **35** (2013), no. 3, C213–C236.
- [26] E. Polizzi, *Density-matrix-based algorithm for solving eigenvalue problems*, Phys. Rev. B **79** (2009), 115112.
- [27] J. Poulson, L. Demanet, N. Maxwell, and L. Ying, *A parallel butterfly algorithm*, SIAM J. Sci. Comput. **36** (2014), no. 1, C49–C65.
- [28] J. Poulson, B. Marker, R. A. van de Geijn, J. R. Hammond, and N. A. Romero, *Elemental: A new framework for distributed memory dense matrix computations*, ACM Trans. Math. Softw. **39** (2013), no. 2, 13:1–13:24.
- [29] Y. Saad and M. H. Schultz, *GMRES: a generalized minimal residual algorithm for solving nonsymmetric linear systems*, SIAM J. Sci. Statist. Comput. **7** (1986), 856–869.
- [30] M. P. Teter, M. C. Payne, and D. C. Allan, *Solution of Schrödinger's equation for large systems*, Phys. Rev. B **40** (1989), 12255–12263.
- [31] L. Ying, *Sparsifying preconditioner for pseudospectral approximations of indefinite systems on periodic structures*, Multiscale Model. Simul. **13** (2015), no. 2, 459–471.
- [32] L. Ying, *Sparsifying preconditioner for the Lippmann-Schwinger equation*, Multiscale Model. Simul. **13** (2015), no. 2, 644–660.
- [33] Y. Zhou, J. R. Chelikowsky, X. Gao, and A. Zhou, *On the “preconditioning” function used in planewave DFT calculations and its generalization*, Commun. Comput. Phys. **18** (2015), 167–179.
- [34] Y. Zhou, Y. Saad, M. L. Tiago, and J. R. Chelikowsky, *Self-consistent-field calculations using Chebyshev-filtered subspace iteration*, J. Comput. Phys. **219** (2006), no. 1, 172–184.

DEPARTMENT OF MATHEMATICS, DEPARTMENT OF PHYSICS, AND DEPARTMENT OF CHEMISTRY, DUKE UNIVERSITY,
BOX 90320, DURHAM NC 27708, USA

E-mail address: jianfeng@math.duke.edu

DEPARTMENT OF MATHEMATICS, DUKE UNIVERSITY, BOX 90320, DURHAM NC 27708, USA

E-mail address: haizhao@math.duke.edu